

The electrical properties of polycrystalline silicon films

John Y. W. Seto

Citation: [Journal of Applied Physics](#) **46**, 5247 (1975); doi: 10.1063/1.321593

View online: <http://dx.doi.org/10.1063/1.321593>

View Table of Contents: <http://scitation.aip.org/content/aip/journal/jap/46/12?ver=pdfcov>

Published by the [AIP Publishing](#)

Articles you may be interested in

[Electrical and structural properties of polycrystalline silicon](#)

J. Appl. Phys. **87**, 7913 (2000); 10.1063/1.373475

[Relationship between electrical properties and structure in uniaxially oriented polycrystalline silicon films](#)

J. Appl. Phys. **71**, 1462 (1992); 10.1063/1.351239

[Electrical conduction mechanism and breakdown property in sputter-deposited silicon dioxide films on polycrystalline silicon](#)

J. Appl. Phys. **65**, 210 (1989); 10.1063/1.342573

[Electrical, thermoelectric, and optical properties of strongly degenerate polycrystalline silicon films](#)

J. Appl. Phys. **56**, 1701 (1984); 10.1063/1.334160

[Transport properties of polycrystalline silicon films](#)

J. Appl. Phys. **49**, 5565 (1978); 10.1063/1.324477

This is a promotional banner for the journal AIP APL Photonics. On the left, there is a small image of the journal's cover, which features a blue and yellow abstract design. To the right of the cover is a yellow starburst graphic with the words 'OPEN ACCESS' in red. The main text of the banner reads 'Launching in 2016!' in a large, white, sans-serif font, followed by 'The future of applied photonics research is here' in a smaller, white, sans-serif font. In the bottom right corner, the 'AIP | APL Photonics' logo is displayed in white. The background of the banner is a vibrant orange with a bokeh effect of light spots.

The electrical properties of polycrystalline silicon films

John Y. W. Seto

Electronics Department, GM Research Laboratories, Warren, Michigan 48090
(Received 14 July 1975)

Boron doses of 1×10^{12} – $5 \times 10^{15}/\text{cm}^2$ were implanted at 60 keV into 1- μm -thick polysilicon films. After annealing at 1100°C for 30 min, Hall and resistivity measurements were made over a temperature range -50–250°C. It was found that as a function of doping concentration, the Hall mobility showed a minimum at about $2 \times 10^{18}/\text{cm}^3$ doping. The electrical activation energy was found to be about half the energy gap value of single-crystalline silicon for lightly doped samples and decreased to less than 0.025 eV at a doping of $1 \times 10^{19}/\text{cm}^3$. The carrier concentration was very small at doping levels below $5 \times 10^{17}/\text{cm}^3$ and increased rapidly as the doping concentration was increased. At $1 \times 10^{19}/\text{cm}^3$ doping, the carrier concentration was about 90% of the doping concentration. A grain-boundary model including the trapping states was proposed. Carrier concentration and mobility as a function of doping concentration and the mobility and resistivity as a function of temperature were calculated from the model. The theoretical and experimental results were compared. It was found that the trapping state density at the grain bound was $3.34 \times 10^{12}/\text{cm}^2$ located at 0.37 eV above the valence band edge.

PACS numbers: 73.60.F, 73.20.H, 72.20.F

INTRODUCTION

The electrical properties of polycrystalline silicon (polysilicon) films prepared by thermal decomposition of silane and doped by diffusion or during growth have been reported by various researchers.^{1–4} In some of these experiments only the dopant-to-silicon atomic ratio in the gas phase was known. In others, the doping concentration was assumed to be the same as the carrier concentration of the epitaxial single-crystalline silicon prepared at the same time or under the same conditions. This appeared to be a reasonable assumption. However, there is still doubt as to what was the actual doping concentration. When experimental results are to be compared with theory, it is important that the impurity concentration be known precisely. In the present work, this is accomplished by using ion implantation. Hall measurements were reported by Kamins⁴ and Cowher and Sedgwick³ but their results were not in good agreement with each other. Neither Hall effect nor resistivity vs temperature have previously been measured or calculated for polysilicon films, although Muñoz *et al.*⁵ performed such measurements on undoped bulk polysilicon rods.

Here we report the results of our electrical measurements on polysilicon films ion implanted with boron so that the doping concentration could be precisely controlled. We made Hall and resistivity measurements over a wide range of temperatures on polysilicon films doped from 1×10^{16} to $5 \times 10^{19}/\text{cm}^3$. A theoretical model is proposed and detailed calculations of the electrical transport properties of polysilicon are compared with experimental results.

EXPERIMENT

The polysilicon films were intentionally prepared undoped by thermal decomposition of silane in argon onto a layer of approximately 3000 Å of silicon dioxide which was thermally grown on *p*-type 10- Ω cm (111)-oriented silicon wafers. All polysilicon depositions were done at 650°C in an infrared heated horizontal reactor. The details of the deposition procedure have been reported elsewhere.⁶ The thickness of the polysilicon films used

in this study ranged from 0.99 to 1.12 μm . Boron doses ranging from 1×10^{12} to $5 \times 10^{15}/\text{cm}^2$ were implanted into the polysilicon films at 60 keV energy. The samples were then annealed at 1100°C for 30 min in a dry nitrogen atmosphere. The annealing was intended to eliminate most of the damage produced by the implantation process and to create a uniform impurity distribution in the polysilicon films due to redistribution by diffusion. Hall measurements on successively anodized and stripped samples show that both carrier concentration and mobility were uniformly distributed. After annealing, Hall bar samples were delineated photolithographically. Aluminum was then electron-beam deposited and another photomask and etching was used to define the contacts. The contacts were alloyed at 500°C for 10

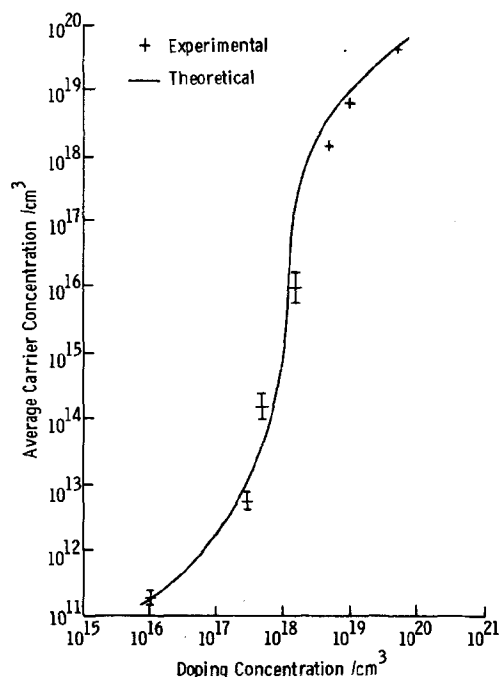


FIG. 1. Comparison of the calculated average carrier concentration vs doping concentration with the room-temperature Hall-measurement data. The solid line is the theoretical curve.

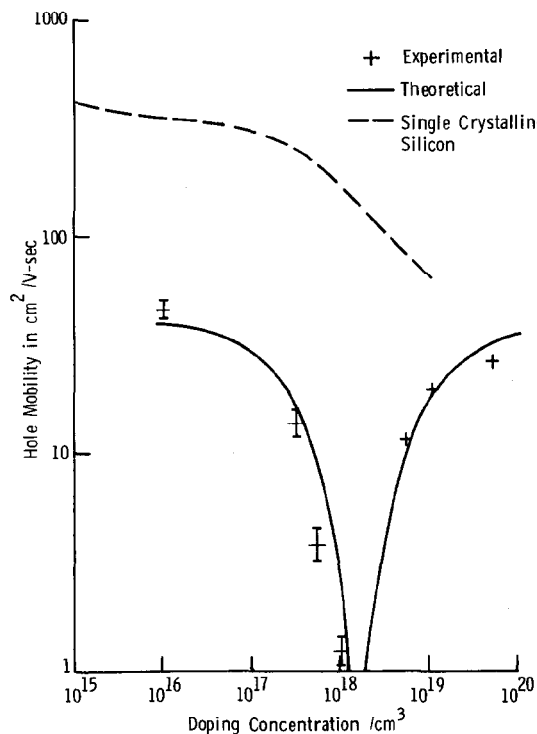


FIG. 2. Room-temperature hole Hall mobility vs doping concentration. The experimental result is plotted together with the theoretical solid curve. The broken line is for single-crystalline silicon.

min to make good Ohmic contacts. Hall measurements were made in magnetic inductions up to 1 T. Hall voltages were always found to be proportional to the applied magnetic field and current through the samples. For each measurement the current polarity was reversed and the Hall voltages in both directions were averaged for calculating the carrier concentration and mobility. In samples doped with less than $5 \times 10^{17}/\text{cm}^3$ of boron, the resistance across the Hall bar was over $10^7 \Omega$ and could be as high as $10^{11} \Omega$. For those samples, the current was supplied by a specially built polyethylene isolated current supply. The Hall voltage was measured by a digital voltmeter buffered by a unity gain electrometer amplifier having an input impedance of $10^{14} \Omega$. When measuring the Hall coefficient and resistivity vs temperature, the sample was mounted on an aluminum block which was enclosed in an aluminum container. The temperature was measured by a thermocouple in direct contact with the back of the polysilicon sample. The whole setup was placed in a temperature chamber. The temperature variation during a measurement was less than $\pm 0.5^\circ\text{C}$.

EXPERIMENTAL RESULTS

Figure 1 is a plot of the carrier concentration vs doping concentration. Since the carriers were found to be uniformly distributed in the film the doping concentration was obtained by dividing the total dose/ cm^2 by the thickness of the polysilicon film. At a doping concentration of $10^{16}/\text{cm}^3$ the carrier concentration is only about $1.8 \times 10^{11}/\text{cm}^3$. As the doping concentration is in-

creased, the carrier concentration remains very small compared to the doping concentration and then increases very rapidly when the doping concentration reaches about $5 \times 10^{17}/\text{cm}^3$. For a doping concentration of $5 \times 10^{18}/\text{cm}^3$ the carrier concentration is approximately 28% of the doping. As the doping concentration is increased further, the carrier concentration approaches that of the doping concentration. Our result is quite similar to that obtained by Cowher and Sedgwick³ who doped their polysilicon films during growth.

The hole mobility in polysilicon and in single-crystalline silicon as a function of doping concentration are plotted in Fig. 2. The most prominent feature in Fig. 2 is the mobility minimum at a doping concentration slightly above $1 \times 10^{18}/\text{cm}^3$. As the doping is increased above $1 \times 10^{19}/\text{cm}^3$ the mobility approaches that in single-crystalline silicon. For doping less than $1 \times 10^{18}/\text{cm}^3$, the mobility increases as the doping is decreased but the mobility is always much smaller than that in single-crystalline silicon. Our over-all result is very much like that of Cowher and Sedgwick.³ However, the mobility of their lightly doped samples was much higher, while the mobility of the heavily doped samples was smaller than this work. Figure 3 is a plot of the room-temperature resistivity as a function of doping. The resistivity reached $10^6 \Omega \text{ cm}$ for lightly doped samples. Increasing the doping from about $1 \times 10^{18}/\text{cm}^3$ results in an abrupt resistivity drop of about five orders of magnitude for only a factor of 10 further increase in doping concentration. Beyond that range the resistivity decreases almost linearly for further increase in doping. The abrupt decrease in resistivity is the result of the increase in carrier concentration and mobility as shown in Figs. 1 and 2.

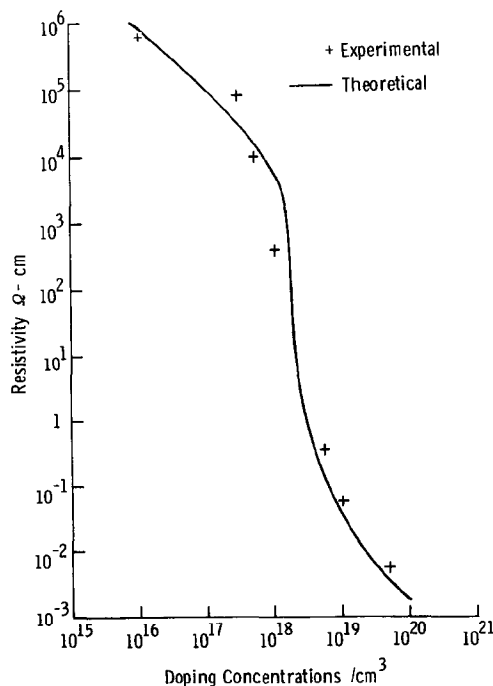


FIG. 3. Room-temperature resistivity vs doping concentration. The experimental data is plotted with theoretical curve.

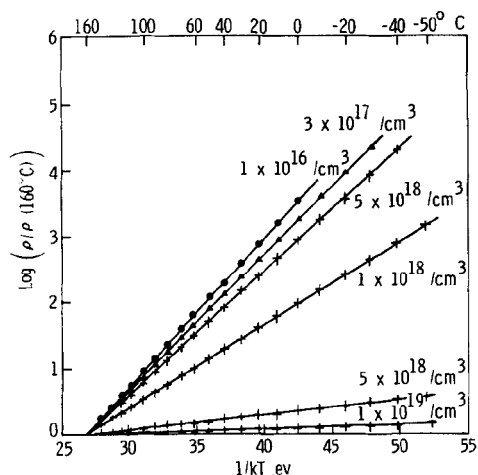


FIG. 4. Logarithm of resistivity vs $1/kT$ for samples with different doping concentrations. The resistivity is normalized by the resistivity at 160°C .

Figure 4 is a logarithmic plot of resistivity normalized by the resistivity at 160°C vs $1/kT$. A linear dependence on $1/kT$ is observed for all samples doped from 1×10^{16} to $1 \times 10^{19}/\text{cm}^3$. The slopes of the curves decrease as the doping was increased. The rate of decrease of the slope as a function of doping was highest at a doping concentration around $1 \times 10^{18}/\text{cm}^3$. As an example, the difference in slopes between samples doped at 1×10^{16} and $3 \times 10^{17}/\text{cm}^3$ is about 0.07 eV ; the difference between 5×10^{18} and $1 \times 10^{19}/\text{cm}^3$ is about 0.03 eV ; but the difference between 1×10^{18} and $5 \times 10^{18}/\text{cm}^3$ is 0.25 eV . The slopes of the lightly doped samples are approximately equal to the half-energy-gap value of single-crystalline silicon. Figure 5 shows hole Hall mobility as a function of $1/kT$ for four samples. For the samples doped 1×10^{18} and $5 \times 10^{18}/\text{cm}^3$ the experimental data yield straight lines having slopes of 0.15 and 0.0335 eV , respectively. For samples doped 1×10^{19} and $5 \times 10^{19}/\text{cm}^3$ the data deviate from straight lines. The mobility of the $5 \times 10^{19}/\text{cm}^3$ doped sample decreases as the temperature is raised, while all the other samples showed increased mobility with temperature.

THEORY

A polycrystalline material is composed of small crystallites joined together by grain boundaries. The angle between the orientations of the adjoining crystallites is often large. Inside each crystallite the atoms are arranged in a periodic manner so that it can be considered as a small single crystal. The grain boundary is a complex structure, usually consisting of a few atomic layers of disordered atoms. Atoms in the grain boundary represent a transitional region between the different orientations of neighboring crystallites. There are two schools of thought concerning the effects of the grain boundary upon the electrical properties of doped polycrystalline semiconductors. One school³ believes that the grain boundary acts as a sink for impurity atoms due to impurity segregation at the grain boundary. Consequently, the amount of impurity in the crystallite is reduced, which leads to a much smaller carrier concentration than the uniformly distributed impurity con-

centration. The carrier concentration does not approach that of the doping concentration until the grain boundary is saturated with impurity atoms. It was also suggested⁵ that segregation of impurity caused the grain interiors to have higher resistance than the grain boundaries. However, it has been shown⁷ that segregation of boron at the grain boundary is significant only at extremely heavily doped concentrations of silicon, e.g., $1.3 \text{ at. } \%$ of boron. No segregation was observed for doping as high as $1.3 \times 10^{20}/\text{cm}^3$.⁷ If the reduction of carriers is the result of impurity segregation at the grain boundary, it is expected that the carrier concentration reduction would depend on the impurity element. It was observed⁴ that both boron and phosphorus behaved similarly in polysilicon. It is also difficult to explain how impurity segregation can lead to the mobility minimum seen in Fig. 2.

The other school of thought^{2,4} reasons that since the atoms at the grain boundary are disordered, there are a large number of defects due to incomplete atomic bonding. This results in the formation of trapping states. These trapping states are capable of trapping carriers and thereby immobilizing them. This reduces the number of free carriers available for electrical conduction. After trapping the mobile carriers the traps become electrically charged, creating a potential energy barrier which impedes the motion of carriers from one crystallite to another, thereby reducing their mobility. Based on this model, for the same amount of doping, the mobility and carrier concentration of a polycrystalline semiconductor would be less than that of a single-crystalline material. Kamins⁴ used this model to explain some of the trends observed in his Hall-effect data. He attributed the decrease in mobility with decreasing carrier concentration to the effect of the high-resistivity space-charge region surrounding the grain

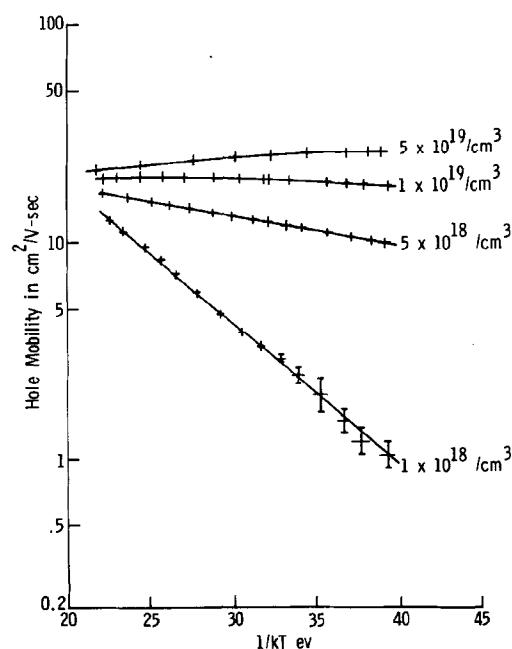


FIG. 5. Hole Hall mobility vs $1/kT$ for samples with different doping concentrations.

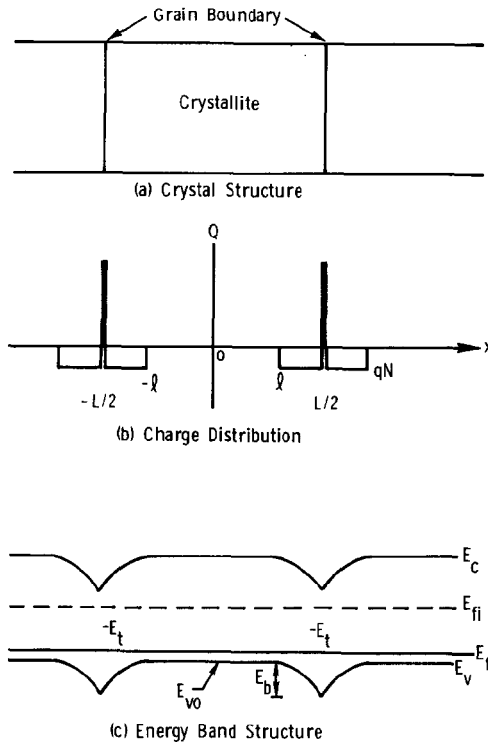


FIG. 6. (a) Model for the crystal structure of polysilicon films. (b) The charge distribution within the crystallite and at the grain boundary. (c) The energy band structure for polysilicon crystallites.

boundary. Choudhury and Hower² used the same model and treated the potential energy barrier as a parameter to explain their measurements of resistivity vs doping concentration.

We believe that the electrical transport properties of polysilicon films are governed by carrier trapping at the grain boundary. In a real polycrystalline material, the crystallites have a distribution of sizes and irregular shapes. To simplify the model we assume that polysilicon is composed of identical crystallites having a grain size of L cm. We also assume that there is only one type of impurity atom present, the impurity atoms are totally ionized, and uniformly distributed with a concentration of N/cm^3 . The single-crystalline silicon energy band structure is also assumed to be applicable inside the crystallites. We further assume that the grain boundary is of negligible thickness compared to L and contains Q_t/cm^2 of traps located at energy E_t with respect to the intrinsic Fermi level. The traps are assumed to be initially neutral and become charged by trapping a carrier. Using the above assumptions an abrupt depletion approximation is used to calculate the energy band diagram in the crystallites. In this approximation, Fig. 6 shows that all the mobile carriers in a region of $(\frac{1}{2}L - l)$ cm from the grain boundary are trapped by the trapping states, resulting in a depletion region. The mobile carriers in the depletion region are neglected in this calculation. Although polysilicon is a three-dimensional substance, for the purpose of calculating its transport properties, it is sufficient to treat the problem in one dimension. Using the above approxi-

mation, Poisson's equation becomes

$$\frac{d^2V}{dx^2} = \frac{qN}{\epsilon}, \quad l < |x| < \frac{1}{2}L, \quad (1)$$

where ϵ is the dielectric permittivity of polysilicon. Integrating Eq. (1) twice and applying the boundary conditions that $V(x)$ is continuous and dV/dx is zero at $x=l$ gives

$$V(x) = (qN/2\epsilon)(x-l)^2 + V_{v0}, \quad l < |x| < \frac{1}{2}L, \quad (2)$$

where V_{v0} is the potential of the valence band edge at the center of the crystallite. Throughout this calculation the intrinsic Fermi level is taken to be at zero energy and energy is positive towards the valence band (the energy band diagram for holes).

For a given crystallite size, there exist two possible conditions depending on the doping concentration: (a) $LN < Q_t$, and (b) $Q_t < LN$.

We first consider the case for $LN < Q_t$. Under this condition, the crystallite is completely depleted of carriers and the traps are partially filled, so that $l=0$ and Eq. (2) becomes

$$V(x) = V_{v0} + (qN/2\epsilon)x^2, \quad |x| \leq \frac{1}{2}L. \quad (3)$$

The potential barrier height, V_B , is the difference between $V(0)$ and $V(\frac{1}{2}L)$, i.e.,

$$V_B = qL^2N/8\epsilon \quad (4)$$

showing that V_B increases linearly with N . Using Boltzmann statistics, the mobile carrier concentration, $p(x)$, becomes

$$p(x) = N_v \exp\{-[qV(x) - E_f]/kT\}, \quad (5)$$

where N_v is the density of states and E_f is the Fermi level. The average carrier concentration, P_a , is obtained by integrating Eq. (5) from $-\frac{1}{2}L$ to $\frac{1}{2}L$ and dividing by the grain size. The result is

$$P_a = \frac{n_i}{Lq} \left(\frac{\pi 2\epsilon kT}{N} \right)^{1/2} \exp\left(\frac{E_B + E_f}{kT}\right) \text{erf}\left[\frac{qL}{2} \left(\frac{N}{2\epsilon kT} \right)^{1/2}\right], \quad (6)$$

where

$$E_B = qV_B \quad (6')$$

and

$$n_i = N_v \exp(-\frac{1}{2}E_g/kT) \quad (6'')$$

is the intrinsic hole concentration of single-crystalline silicon (with band gap E_g) at temperature T .

In Eq. (6), the Fermi level is determined by equating the number of carriers trapped to the total number of trapping states occupied, given as

$$LN = \frac{Q_t}{2 \exp[(E_t - E_f)/kT] + 1} \quad (7)$$

The traps are considered to be identical; each trap is capable of trapping only one hole of either spin; and there is no interaction between traps. From Eq. (7), the Fermi level is given as

$$E_f = E_t - kT \ln[\frac{1}{2}(Q_t/LN - 1)]. \quad (8)$$

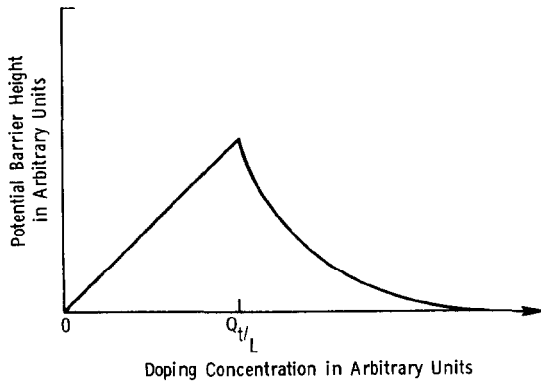


FIG. 7. Functional dependence of the potential barrier height on doping concentration.

With Eqs. (6) and (8), the carrier concentration can be calculated for a given N , if L , Q_t , and E_t are known. A method of obtaining these values will be discussed later.

If $LN > Q_t$ only part of the crystallite is depleted of carriers and $l > 0$. The potential barrier height then becomes [from Eq. (2)]

$$V_B = qQ_t^2/8\epsilon N. \quad (9)$$

Using Eqs. (4) and (9), a plot of V_B as a function of doping concentration is shown in Fig. 7. It is noted that as the doping concentration is increased, the potential barrier at first increases linearly, reaching a maximum at $LN = Q_t$, then decreases rapidly as $1/N$. This behavior results from the dipole layer created when impurity atoms are first introduced and the traps are being filled. The strength of the dipole layer increases as more impurity atoms are added. However, after all the traps are filled, the total charge in the dipole remains the same but the width of the dipole layer is decreased and the potential barrier decreases. The average carrier concentration, p_a , is obtained as before, by averaging over the crystallite. In the undepleted region, the carrier concentration, p_b , is the same as that of a similarly doped single-crystalline silicon,

$$p_b = N_v \exp[-(E_{v0} - E_f)/kT] \quad (10)$$

for a nondegenerately doped sample. The carrier concentration in the depletion region is given in Eq. (5). The average carrier concentration, p_a , can be shown to be

$$p_a = p_b \left\{ \left(1 - \frac{Q_t}{LN}\right) + \frac{1}{qL} \left(\frac{2\epsilon kT\pi}{N}\right)^{1/2} \operatorname{erf} \left[\frac{qQ_t}{2} \left(\frac{1}{2\epsilon kTN}\right)^{1/2} \right] \right\}. \quad (11)$$

The resistance of a polycrystalline material consists of the contributions from the grain-boundary region and the bulk of the crystallite. If the conduction in the crystallite is much higher than that through the grain boundary, it is a good approximation to consider just the resistance of the grain-boundary region. There are two important contributions to the current across the grain boundary: thermionic emission and tunneling (field emission). Thermionic emission results from those

carriers possessing high enough energy to surmount the potential barrier at the grain boundary. On the other hand, the tunneling current arises from carriers with energy less than the barrier height. These carriers go through the barrier by quantum-mechanical tunneling.

When the barrier is narrow and high, the tunneling current can become comparable to or larger than the thermionic emission current. In polysilicon the potential barrier is highest when the barrier width is the widest. The barrier height decreases rapidly to a small value for a highly doped polysilicon, therefore, the tunneling current is always expected to be smaller than the thermionic emission current. Because of this, tunneling current will be neglected in our calculation. Following Bethe,⁸ the thermionic emission current density, J_{th} , for an applied voltage, V_a , across a grain boundary is

$$J_{th} = q\bar{p}_a \left(\frac{kT}{2m^*\pi}\right)^{1/2} \exp\left(-\frac{qV_B}{kT}\right) \left[\exp\left(\frac{qV_a}{kT}\right) - 1\right], \quad (12)$$

where m^* is the effective mass of the carrier. Equation (12) was obtained by neglecting collisions within the depletion region and the carrier concentration in the crystallite was assumed to be independent of the current flow, so that it is applicable only if the number of carriers taking part in the current transport is small compared to the total number of carriers in the crystallite. This condition restricts the barrier height to be larger than or comparable to kT . If V_a is small, $qV_a \ll kT$, Eq. (12) can be expanded to give

$$J_{th} = q^2\bar{p}_a \left(\frac{1}{2\pi m^*kT}\right)^{1/2} \exp\left(-\frac{qV_B}{kT}\right) V_a, \quad (13)$$

which is a linear current-voltage relationship. From Eq. (13) the conductivity of a polysilicon film with a grain size L cm is

$$\sigma = Lq^2\bar{p}_a \left(\frac{1}{2\pi m^*kT}\right)^{1/2} \exp\left(-\frac{qV_B}{kT}\right). \quad (14)$$

Inserting Eqs. (6) and (11) into Eq. (14), we find that

$$\sigma \propto \exp[-(\tfrac{1}{2}E_g - E_f)/kT], \quad \text{if } NL < Q_t, \quad (15)$$

$$\sigma \propto T^{-1/2} \exp(-E_B/kT), \quad \text{if } NL > Q_t. \quad (16)$$

Plotting the logarithm of the resistance vs $1/kT$ should give a straight line with a slope equal to $\tfrac{1}{2}E_g - E_f$ if $LN < Q_t$ and E_B if $LN > Q_t$. This interpretation will fail when $E_B \ll kT$, which is likely for highly doped material.

Using the relationship

$$\sigma = qp\mu \quad (17)$$

together with Eq. (14), an effective mobility, μ_{eff} , is given as

$$\mu_{eff} = Lq \left(\frac{1}{2\pi m^*kT}\right)^{1/2} \exp\left(-\frac{E_B}{kT}\right). \quad (18)$$

Since the energy barrier, E_B , exhibits a maximum as a function of doping, Eq. (18) shows that the mobility will have a minimum as a function of doping. The minimum occurs when $LN = Q_t$. Furthermore, a plot of the logarithm of μ_{eff} vs $1/kT$ should yield a straight line with a negative slope of E_B , if $E_B > kT$.

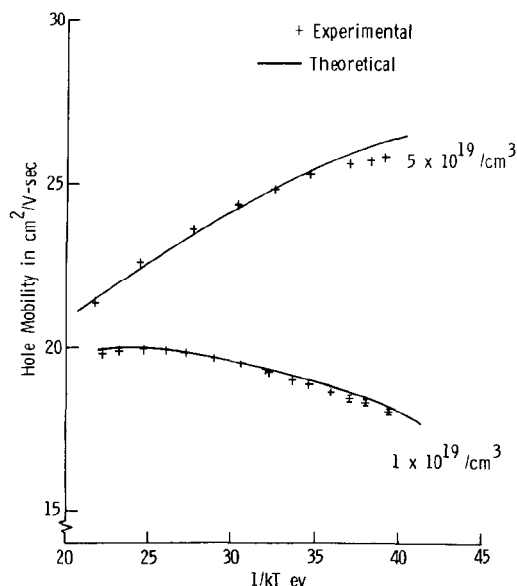


FIG. 8. The experimental hole mobility vs $1/kT$ is compared with the theoretical curve for 5×10^{19} and $1 \times 10^{19}/\text{cm}^3$ doping using potential barrier heights of 0.005 and 0.022 eV, respectively.

COMPARISON WITH EXPERIMENT

The above results can be summarized as (a) the carrier concentration of polysilicon is very small for $LN < Q_t$ and increases abruptly as LN approaches Q_t , then for further increase in doping concentration the carrier concentration asymptotically approaches that of the carrier concentration of a single-crystalline silicon with the same amount of doping; (b) the conductivity and mobility of polysilicon vary as $\exp(-E_B/kT)$ for $E_B > kT$; (c) the mobility as a function of doping concentration exhibits a minimum when $N = Q_t/L$.

In this theory there are three parameters: the grain size, L ; the grain boundary trapping state density, Q_t ; and the trapping state energy level, E_t . The grain size can be observed directly using transmission electron microscopy and image analysis. Such experiments showed that the average grain size for our samples was about 200 Å. Q_t can be obtained from the mobility-vs- $1/kT$ plot and Eqs. (9) and (18). From Fig. 5, the value of E_B for the $5 \times 10^{18}/\text{cm}^3$ sample results directly from the slope of the curve. In the samples doped with 1×10^{19} and $5 \times 10^{19}/\text{cm}^3$ a fitting to Eq. (18) is used to obtain E_B . The values of E_B that give the best fit to the experimental results are 0.022 and 0.005 eV, respectively. The result of the fitting is shown in Fig. 8. Table I lists the values of Q_t for the three samples; they range from 2.98×10^{12} to $3.64 \times 10^{12}/\text{cm}^2$. The average value of Q_t , $3.34 \times 10^{12}/\text{cm}^2$, will be used in our calculation. This value is approximately equal to the value of the surface state density of a single-crystalline silicon. The grain boundary of a polysilicon can probably be considered as composed of two free silicon surfaces in contact. The number of trapping states is thus likely to be close to the surface state density of a free silicon surface. From Fig. 5, the slope of the $1 \times 10^{18}/\text{cm}^3$ sample is 0.15 eV. Since LN is less than Q_t for this

sample, using Eq. (4), L is calculated to be 270 Å, in good agreement with the average value of 200 Å obtained from transmission electron microscope study. The trapping state energy, E_t , can be obtained from Eqs. (6) and (8). It has been shown^{4,9} that for a composite material such as polysilicon, Hall measurements give the carrier concentration within the crystallites if the conductivity of the bulk crystallite is much higher than that of the grain boundary. It has also been shown¹⁰ that if the mobility in the crystallite is not a function of position then the carrier concentration obtained by the Hall measurement is the average value within the crystallite, as given in Eqs. (6) and (11). Therefore, Hall measurements give the average carrier concentrations in the lightly and highly doped polysilicon films. For the intermediately doped film, where $LN \approx Q_t$, the energy bands within the crystallite are very nonuniform and the carrier concentration obtained by the Hall measurement can be significantly different from the average value in the crystallite. To ensure the validity of the experimental data when computing E_t , we use the experimental value at a doping density of $1 \times 10^{16}/\text{cm}^3$, the lowest doping used in our experiment. Using Eqs. (6) and (8) and the measured carrier concentration of $1.8 \times 10^{11}/\text{cm}^3$ the trapping state energy is found to be 0.37 eV above the valence band edge. Dumin¹¹ found a deep level in silicon on sapphire at 0.3 eV above the valence band edge. It is possible that this level might be of the same origin as that in polysilicon films.

Using these values of L , Q_t , and E_t the theoretical carrier concentration vs doping concentration is plotted as a solid line in Fig. 1. The experimental and theoretical values are in good agreement. The deviation in the range between 5×10^{17} and $7 \times 10^{18}/\text{cm}^3$ is the result of the rapid rise in carrier concentration as a function of doping so that it is very sensitive to experimental error. Also, as discussed previously, the carrier concentration derived from the Hall measurement can differ significantly from that of the actual average carrier concentration. Figures 2 and 3 are the theoretical hole mobility and resistivity vs doping concentration plotted together with experimental data. In these plots a scaling factor of 0.154 has been applied to Eq. (4) to obtain the theoretical curves. Andrews and Lepselter¹² calculated the effective Richardson's constant for holes in silicon for metal silicide Schottky barriers to be about 0.25 that of free electron. Our value of the effective Richardson's constant is found to be 0.12. This supports our assumption that the hole transport in polysilicon is dominated by thermionic emission. In Fig. 9, the theoretical and experimental values of the activation energy for samples with different doping densities are shown. The experimental activation energies are de-

TABLE I. Trapping state density and energy barrier height for three samples with different doping concentrations.

Doping concentration	Energy barrier, E_B	Trapping state density, Q_t
$5 \times 10^{18}/\text{cm}^3$	0.0335 eV	$2.98 \times 10^{12}/\text{cm}^2$
$1 \times 10^{19}/\text{cm}^3$	0.022 eV	$3.41 \times 10^{12}/\text{cm}^2$
$5 \times 10^{19}/\text{cm}^3$	0.005 eV	$3.64 \times 10^{12}/\text{cm}^2$

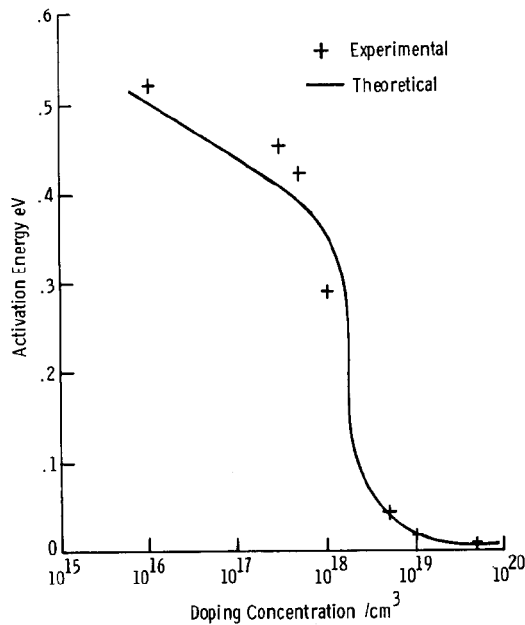


FIG. 9. Comparison of the experimental and theoretical activation energy as a function of doping concentration. The experimental values are derived from Fig. 4.

rived from the slopes of the resistivity-vs- $1/kT$ plot in Fig. 4. The theoretical values are obtained from Eqs. (8), (9), (15), and (16). The energy gap, E_g , in Eq. (15) is taken to be that of single-crystalline silicon. The experimental values of the activation energy is always larger than the theoretical values for lightly doped samples. This is because in our theory the trapping states are assumed to have a δ function distribution, while in real polysilicon the trapping states are distributed over an energy range.¹³ The δ -function approximation causes the Fermi energy to increase much more rapidly as dopants are added to the polysilicon film. This results in a lower calculated activation energy. Otherwise, the theoretical and experimental results are in good agreement.

To compare our theory with previously reported experiments is complicated by the fact that most reports did not indicate the grain size of their samples. This in itself is not a problem because, at worst, the grain size can be treated as a parameter. It was reported that the grain size of polysilicon films changed as the doping concentration and deposition temperature were changed.^{14,15} If the grain size is neither known nor can be treated as a constant a comparison with theory can only provide an indication of the validity of the theory. We compared our theory with the experimental results reported by Kamins⁴ and Cowher and Sedgwick³; a broad agreement between experiment and theory was obtained.

DISCUSSION

We have shown that the barrier model is essentially correct for polysilicon since it gives good agreement between experiment and theory. It reveals the importance of knowing the grain size if theoretical and experimental results are to be compared. Although this

theory has been applied to *p*-type polysilicon, it is equally applicable to *n*-type polysilicon. It has been shown¹⁶ that in *n*-type silicon the grain boundary has an electron trapping level located between the intrinsic Fermi level and the conduction band edge. By performing the type of experiments reported here, a comparison between theory and experiment is possible and the trapping state density and energy can be found.

We now discuss some of the limitations of the model and our calculations. We neglected the contribution to the resistivity by the bulk of the crystallites. This assumption fails if the resistance of the bulk is comparable to that of the barrier. Such a situation is possible if the grain size of the polysilicon film is large and the doping is high as is the case in Kamins's polysilicon⁴ doped above $7 \times 10^{18}/\text{cm}^3$. For those samples it is necessary to take the bulk of the crystallites into account. It has been shown¹³ that the surface states of a free silicon surface are not fixed at a discrete energy but distributed over an energy range. It is likely that the trapping states in the grain boundary of polysilicon are also distributed over an energy range. Such a distribution will modify the calculations since we assumed a δ -function approximation. The effect on the activation energy was discussed in the above section. The effects on mobility and carrier concentration are to cause their changes as a function of doping concentration to be much slower when $LN \approx Q_t$. Unless the distribution spreads to within a few kT of the valence band there should be no effect on the highly doped samples, i.e., $LN \gg Q_t$.

In large grain polysilicon, such as the ones prepared in hydrogen at temperatures around 1000°C and bulk polysilicon rods, the free-carrier concentration in the "depletion layer" can be appreciable. Using the depletion approximation leads to inaccurate values of the barrier heights. The mobility is exponentially dependent on the barrier height, as shown in Eq. (18). Any inaccuracy in the calculated potential barrier height strongly affects the calculated mobility values. The carrier concentration is affected less because the carrier density depends on the shape of the barrier only in the depletion region. The total carrier concentration in the depletion region is usually small compared to the carriers in the nondepleted region. A deviation from the actual barrier shape only causes a small error in the carrier concentration, except when $Q_t \approx LN$. Using the values of Q_t and E_t obtained in our experiment, we estimated that the depletion approximation is good up to a grain size of about 600 Å. Beyond this grain size, a quantitative comparison between experiment and theory is possible only if the free carriers, distribution of the trapping states, and the resistance of the bulk crystallites are taken into account. However, the essential qualitative features of the behavior of the carrier concentration, mobility, and resistivity can be inferred from our calculation.

ACKNOWLEDGMENTS

The author is grateful for the interest in this work by all his colleagues. He would like to thank Dr. M.C. Steele for his encouragement, many helpful discussions, and reading of the manuscript. He appreciates some in-

formative discussions with Dr. T. I. Kamins. Thanks are also due to Mrs. B. Vannoy for her technical assistance and B. MacIver for implanting the samples.

¹A. L. Fripp and L. H. Slack, *J. Electrochem. Soc.* **120**, 145 (1973).

²P. Rai-Choudhury and P. L. Hower, *J. Electrochem. Soc.* **120**, 1761 (1973).

³M. E. Cowher and T. O. Sedgwick, *J. Electrochem. Soc.* **119**, 1565 (1972).

⁴T. I. Kamins, *J. Appl. Phys.* **42**, 4357 (1971).

⁵E. Muñoz, J. M. Boix, J. Llabres, J. P. Mónico, and J. Piqueras, *Solid-State Electron.* **17**, 439 (1974).

⁶J. Y. W. Seto, *J. Electrochem. Soc.* **122**, 701 (1975).

⁷G. L. Pearson and J. Bardeen, *Phys. Rev.* **75**, 865 (1949).

⁸H. A. Bethe, MIT Radiation Laboratory Report No. 43-12, 1942 (unpublished).

⁹J. Volger, *Phys. Rev.* **110**, 1023 (1950).

¹⁰R. L. Petritz, *Phys. Rev.* **110**, 1254 (1958).

¹¹D. J. Dumin, *Solid-State Electron.* **13**, 415 (1970).

¹²S. M. Sze, *Physics of Semiconductor Devices*, (Interscience, New York, 1969).

¹³A. Many, Y. Goldstein, and N. B. Grover, *Semiconductor Surfaces* (Wiley, New York, 1965).

¹⁴F. C. Eversteyn and B. H. Put, *J. Electrochem. Soc.* **120**, 106 (1973).

¹⁵L. H. Hall, K. M. Koliwad, and L. N. Swink, *Thin Solid Films* **18**, 145 (1973).

¹⁶Y. Matukura, *Jpn. J. Appl. Phys.* **2**, 91 (1963).